Comparative Analysis of Methods for Estimating Arm Segment Parameters and Joint Torques From Inverse Dynamics

Davide Piovesan[1]
Robotics Laboratory,
Sensory Motor Performance Program (SMPP),
Rehabilitation Institute of Chicago,
345 East Superior Street,
Suite 1406,
Chicago, IL 60611;
Ashton Graybiel Spatial Orientation Laboratory,
Brandeis University,
Waltham, MA 02454
e-mail: d-piovesan@northwestern.edu

Alberto Pierobon
Ashton Graybiel Spatial Orientation Laboratory,
Brandeis University,
Waltham, MA 02454
e-mail: pierobon@brandeis.edu

Paul DiZio
e-mail: dizio@brandeis.edu

James R. Lackner
e-mail: lackner@brandeis.edu
Ashton Graybiel Spatial Orientation Laboratory,
Brandeis University,
Waltham, MA 02454;
Volen Center for Complex Studies,
Brandeis University,
Waltham, MA 02454

A common problem in the analyses of upper limb unfettered reaching movements is the estimation of joint torques using inverse dynamics. The inaccuracy in the estimation of joint torques can be caused by the inaccuracy in the acquisition of kinematic variables, body segment parameters (BSPs), and approximation in the biomechanical models. The effect of uncertainty in the estimation of body segment parameters can be especially important in the analysis of movements with high acceleration. A sensitivity analysis was performed to assess the relevance of different sources of inaccuracy in inverse dynamics analysis of a planar arm movement. Eight regression models and one water immersion method for the estimation of BSPs were used to quantify the influence of inertial models on the calculation of joint torques during numerical analysis of unfettered forward arm reaching movements. Thirteen subjects performed 72 forward planar reaches between two targets located on the horizontal plane and aligned with the median plane. Using a planar, double link model for the arm with a floating shoulder, we calculated the normalized joint torque peak and a normalized root mean square (rms) of torque at the shoulder and elbow joints. Statistical analyses quantified the influence of different BSP models on the kinetic variable variance for given uncertainty on the estimation of joint kinematics and biomechanical modeling errors. Our analysis revealed that the choice of BSP estimation method had a particular influence on the normalized rms of joint torques. Moreover, the normalization of kinetic variables to BSPs for a comparison among subjects showed that the interaction between the BSP estimation method and the subject specific somatotype and movement kinematics was a significant source of variance in the kinetic variables. The normalized joint torque peak and the normalized root mean square of joint torque represented valuable parameters to compare the effect of BSP estimation methods on the variance in the population of kinetic variables calculated across a group of subjects with different body types. We found that the variance of the arm segment parameter estimation had more influence on the calculated joint torques than the variance of the kinematics variables. This is due to the low moments of inertia of the upper limb, especially when compared with the leg. Therefore, the results of the inverse dynamics of arm movements are influenced by the choice of BSP estimation method to a greater extent than the results of gait analysis. [DOI: 10.1115/1.4003308]

1 Introduction

In biomechanics and motor control, the estimation of the joint torques necessary to perform a movement is a corner stone of muscle force analysis and the study of movement control strategies and proprioception [1–4]. In the case of unfettered movements, measuring the joint torques using torquemeters is impossible, or at least very impractical, as force transducers need to be placed in series with the two interacting bodies, and that would only be possible through surgery in the case of human joints. Alternative insertion methods would require the subject to exert joint torques against an additional load, proper of the device, rather than just moving the arm segments. Hence, the introduction of a measuring apparatus would automatically interfere with the goal. For this reason, inverse dynamics analyses are the preferred estimation tools, even though such methods can be affected by errors deriving from several different sources.

Planar arm movements are of particular interest. Restricting the arm range of motion within the horizontal plane allows researchers the use of a biomechanical model with a low number of degrees of freedom (DOFs), which results in a reduced dimensionality of the inverse dynamics problem. The inputs for inverse dynamics equations are the kinematic variables measured during the task and the body segment parameters (BSPs) such as mass (M), center of mass location (CM), and moment of inertia (IM) [2,5]. The measure of kinematics is generally a direct measure done in vivo with several methods. Depending on the method used, the errors that can affect the measured kinematics are due to (1) inaccuracy of the transducers, (2) movement artifacts generated by the wobbling of soft tissue, and (3) numerical errors due to calculation of derivatives [5–12]. In addition to filtering techniques to reduce high frequency noise, there are several correction methods that are still in development, such as marker clusters [13] or joint constraint optimizations [14–16]. On the other hand, accurate estimations of body segment parameters are particularly difficult to obtain in vivo and are seldom the result of direct measure [17]. Postprocessing corrections of the estimations, such as probabilistic approaches [18] or numerical optimizations [19,20], seem promising but are seldom used. Hence, it is common practice to estimate BSP using regression equations. Estimations can be obtained from different approaches and assumptions. Several

[1]Corresponding author.

Contributed by the Bioengineering Division of ASME for publication in the JOURNAL OF BIOMECHANICAL ENGINEERING. Manuscript received August 5, 2009; final manuscript received December 20, 2010; published online February 4, 2011. Assoc. Editor: Richard Neptune.

studies on cadavers employed statistical relationships to correlate the geometry of the limb with BSPs of different populations. Yet, regression equations based on cadavers are usually obtained from a rather small sample population, and the loss of fluid in the body segments during measure can affect the accuracy of the estimations [21–25]. Other methods estimate BSPs by approximating the limb segments' geometry and volume either using simple geometrical shapes [26,27] or more accurately through photogrammetry [28–32] or water immersion [33,34], assuming that the density of tissues is constant and invariable among subjects. More complete studies estimate BSPs from the geometry of the limbs and the density distribution measured from energy absorption during irradiation with different sources (gamma ray, X-ray, and magnetic resonance imaging (MRI)) [35–39].

While sensitivity analyses on the inverse dynamics calculations have been extensively studied in gait, posture, and single joint movements [7,8,14,18–20,40–49], there are no comprehensive statistical analyses performed on multijoint reaching movements. Studies concerning reach to grasp movements pose an additional challenge, as it has been observed that the shape of the hand tends to change within 120 ms after the onset of the movement when reaching for differently shaped objects [50]. Current methods to estimate BSPs do not extend to different configurations of the hand; thus, an average shape must be chosen.

Previous work on sensitivity analysis, applied to inverse dynamics of gait, explored the effect of a percentage variation of each body segment parameter independently. However, M, CM, and IM are clearly correlated with one another. Furthermore, although the effects of BSPs and subject somatotype on the estimation of kinetic variables are often considered independent, an interaction could occur [18,29,51] and can be explained by the sensitivity of BSP estimation methods to differences in somatotype (sturdy, slender, etc.).

The purpose of this study was to statistically and analytically quantify the influence of different sources of uncertainty and their interactions on the variance of the kinetic variables at the shoulder and elbow joints during fast nonballistic arm reaching movements. Particular attention was paid to the influence of the shape of the hand. Specifically, methods that modeled the hand as completely extended were compared with methods that assume the hand in other configurations.

2 Methods

Thirteen subjects (ten males and three females; age: 32 ± 14 years, mass: 78 ± 15 kg, height: 1.75 ± 0.09 m, and mean $\pm$ SD%) gave informed consent to participate in the study, which was approved by Brandeis IRB. We estimated the BSPs of the subjects' right upper limb using eight sets of commonly employed regression equations and a water-displacement method (PI) [33,34].

The first method, proposed by Hanavan (HV) [26], is based on the approximation of the geometry of the limb with 3D basic geometric shapes. The second method, proposed by McConville (MC), determined the geometric properties of the arm from in vivo photographic images [28]. The third and fourth methods, proposed by Zatsiorsky and Seluyanov (Z1, Z2), are based on in vivo scans, performed using gamma rays, to determine the distribution of density [38,39]. The fifth method, proposed by de Leva (DL), is an adjustment of the previous two, considering a slightly different segmentation of the arm [52]. The last three methods, proposed by Dempster (DE), Chandler (CH), and Clauser (CL), respectively, derived the regression equations from cadavers [21–23,25,53]. Moment of inertia values for the method proposed by Clauser were extracted from Winter's review [2]. Each model suggested a series of limb and anthropometric dimensions to input in the equations required to obtain the inertial data. The evident difference among the methods was most pronounced in the modeling of the shape of the hand: Hanavan approximated the hand with a sphere, Dempster defined it as "fist-shaped," Clauser assumed the hand to be flexed to approximately 30 deg with the fingers slightly curled in a relaxed position, and Chandler defined the position of the hand as "relaxed." McConville, de Leva, the two methods of Zatsiorsky, and the water immersion method assumed the hand to be in complete extension.

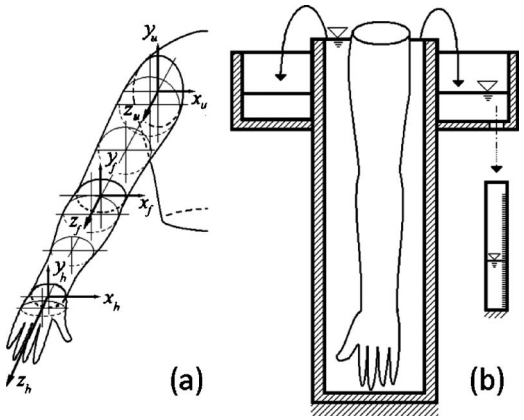

Fig. 1 (*a*) Upper arm, forearm, and hand segmentation employed in our (PI) estimation method. Each section was divided in portions with length up to 0.1 m starting from the distal end. The moment of inertia IM of each portion was measured about the *y*-axes and combined in the matrix of inertia of the complete limb by means of the Huygens–Steiner theorem. (*b*) Apparatus used to measure the volume of the portions. The water was warmed to a temperature of 37°C for comfort. A graduated cylinder with a resolution of 2×10^{-7} m^3 was used to measure the volume of water progressively displaced by each portion. The graduated cylinder was emptied after the immersion of each portion.

To compute BSPs using the water immersion method, each subject's right arm was divided into three main sections: hand, forearm, and upper arm (as also suggested in all the estimation methods above). The length of the hand was measured as the distance between the tip of the fingernail of the middle-finger and the styloid process (with the hand flat on a surface to avoid flexion of the fingers). Lengths of the forearm and upper arm were measured as the distance between the styloid process and the olecranus lateral epicondyle and the distance between the olecranus lateral epicondyle and the humerus great tuberosity, respectively. Each section's main reference frame origin was placed at the center of the proximal extremity: With the arm extended and parallel to the transversal plane (plane of movement), z_k-axis was aligned longitudinally with the distal positive direction, x_k-axis parallel to the transverse plane and positive in the medial direction, and y_k-axis parallel to the frontal plane and positive in the ventral direction. Each section was subdivided into portions of up to 0.1 m in length (Fig. 1(*a*)). We measured the dimensions along x_k and y_k and the perimeters of the base, center, and upper edge of each portion.

The apparatus we used to measure the volume of the arm consisted of a cylinder filled with water up to the top ridge. We measured the water volume overflowing when each portion of the arm sections was gradually immersed in the cylinder (Fig. 1(*b*)). This volume was then used to calculate BSPs knowing the geometry of each portion and assuming a uniform density and percentage of tissue distribution as given by Clarys and Marfell-Jones [54,55]. All moments of inertia in the results were computed about the axis of inertia centered on CM and orthogonal to the plane of movement. Subsequently, using the Huygens–Steiner theorem, we calculated the moment of inertia of each segment with respect to its proximal end in order to compute IM about the wrist joint for the hand, about the elbow joint for the forearm, and about the shoulder joint for the upper arm.

2.1 Movement Task. Many experiments on upper limb focus

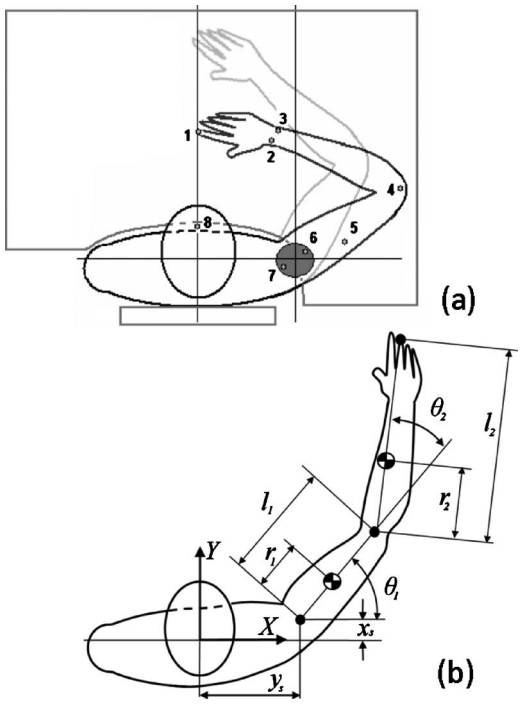

Fig. 2 (*a*) **Position of Optotrak® active markers: (1) index finger tip, (2) styloid process of radius, (3) head of ulna, (4) lateral epicodyle of humerus, (5) deltoid tuberosity, (6) greater tubercle of humerus, (7) acromion, and (8) manubrium of sternum. The shape of the table was such as to restrain the movement of the subjects' torso, minimizing the translation of the shoulder centroid (x_s, y_s).** (*b*) **Variables used in the floating base double-pendulum planar model. X denotes the medial-lateral direction and Y the dorso-ventral direction. An Optotrak® system was used to measure the constants l_1 and l_2, the coordinates of the shoulder centroid (x_s, y_s), and the angles θ_1 and θ_2 during the movement. The positions of r_1 and r_2 were calculated for each estimation method.**

on the analysis of proprioceptive feedback. Hence, the visual feedback of the subject is often precluded, causing increased variability in the kinematics both within and across subjects [56–58]. To take into account this particular aspect of the upper limb studies, the experiment was conducted in complete darkness. The subject was seated at a table. The seat height was adjusted for each subject to keep the arm trajectory planar, allowing a maximum of 0.2 m between the table surface and the acromion. To limit the movement of the torso, the subject was restrained between the edge of the table and the back of the chair (Fig. 2(*a*)). Two light-emitting diodes (LEDs) placed under the semitransparent plastic surface of the table were used as starting point and goal target. During the movement, the goal light stayed on, and the intensity of the light was sufficient to localize the target, but not to see the trajectory of the hand. Each subject was asked to lift his/her elbow from the table while touching the starting point with his/her extended index finger and wait until the goal target was lighted, at which point the subject had to reach and touch the location of the goal target in one continuous fast, nonballistic natural movement (duration of 500 ± 35 ms), similar to picking up an object on the table (peak velocities of 2.53 ± 0.17 rad/s for the elbow joint and 1.05 ± 0.09 rad/s for the shoulder). Contact with the surface of the workspace was allowed only at the starting and target points. If subjects reported any surface contact during the reaching movement, the trial was discarded. The planarity of the movement and position of the shoulder centroid was recorded and is reported in Sec. 3. After four training sessions of eight reaches, each subject performed a total of 72 reaching movements (12 sets of six reaches). Verbal feedback was given to help the subject maintain similar movement duration.

The starting point and the goal target were in a straight line on the medial plane and parallel to the horizontal plane. To maintain congruence across subjects of the start and finish joint angles and their variation during the reaching movements, the placement of the starting and goal positions along the line was varied for each subject. This was possible because a proportionality exists among the average medial-lateral distance between the sternum and the average center of rotation of the humerus ($\bar{y}_s$), the upper-arm length (l_1), and the sum of forearm and hand lengths (l_2). In particular, the ratio l_1/l_2 is a constant equal to 0.73 ± 0.02 (Fig. 2(*b*)). We obtained average angular displacements of 1.13 ± 0.09 rad for the elbow joint and 0.61 ± 0.05 rad for the shoulder. This arrangement allowed us to minimize the variability of angular kinematic of elbow and shoulder joints across subjects.

Three-dimensional movement kinematics were measured with a three-sensor Optotrak® motion capture system (model 3020, Northern Digital Inc., Waterloo, Ontario, Canada) and sampled at 200 Hz. Eight active markers were placed on the subjects' right arm and sternum (Fig. 2(*a*)).

The three-dimensional accelerations of the hand were also measured with three single-axis accelerometers (Kistler, 8352A-10M3) placed on a very light mounting bracket on the radial styloid process. The signal was sampled at 4000 Hz after anti-aliasing filtering at 1024 Hz with a four pole Butterworth filter. The mount was part of a rigid brace used to constrain the flexion of the wrist during movement so to simplify the biomechanical modeling.

2.2 Biomechanical Model. A planar, two-link mechanical model was used for the arm. Kinematics and dynamics were described in a Cartesian coordinate system where on the horizontal plane, the x-axis was positive in the lateral direction and the y-axis was positive in the frontal direction, and on the vertical plane, the z-axis completed a right handed frame [59–62]. Subscript "1" referred to variables of the upper-arm link and shoulder joint, while subscript "2" identified forearm-hand link and elbow joint variables. Therefore, θ_1 and θ_2 were the shoulder and elbow angles, respectively, r_1 was the distance between the upper-arm CM and the shoulder joint, while r_2 was the distance between the forearm-hand CM and the elbow joint (Fig. 2(*b*)).

Inverse dynamics calculation accounted for the translation of the shoulder [63]. Gravity did not influence the joint torque since it was acting orthogonally to the arm trajectory:

$$\begin{cases} \tau_1 = \tau_2 + m_1 \cdot r_1 \cdot (\ddot{\bar{y}}_1 c_1 - \ddot{\bar{x}}_1 s_1) + m_2 \cdot l_1 \cdot (\ddot{\bar{y}}_2 c_1 - \ddot{\bar{x}}_2 s_1) + I_{z1}(\ddot{\theta}_1) \\ \tau_2 = m_2 \cdot r_2 \cdot (\ddot{\bar{y}}_2 c_{12} - \ddot{\bar{x}}_2 s_{12}) + I_{z2}(\ddot{\theta}_1 + \ddot{\theta}_2) \end{cases} \tag{1}$$

where τ_i were the joint torques exerted by the muscle to accomplish the movement, $(\bar{x}_i, \bar{y}_i)$ with the links' CM coordinates, I_{zi} were the moments of inertia about the z-axis calculated at the links' center of mass, $s_i = \sin(\theta_i)$, $s_{ij} = \sin(\theta_i + \theta_j)$, and similarly for c_i and c_{ij}.

The coordinates of the center of mass can be extracted from Fig. 2(*b*), where (x_s, y_s) account for the nonholonomic translation of the shoulder:

$$\begin{aligned} \bar{x}_1 &= r_1 c_1 + x_s \\ \bar{y}_1 &= r_1 s_1 + y_s \\ \bar{x}_2 &= l_1 c_1 + r_2 c_{12} + x_s \\ \bar{y}_2 &= l_1 s_1 + r_2 s_{12} + y_s \end{aligned} \tag{2}$$

Equation (1) can be rewritten in a matrix form by calculating the second derivative of Eq. (2) with respect to time and substituting

$$\begin{bmatrix} \alpha + 2\beta c_2 & \delta + \beta c_2 \\ \delta + \beta c_2 & \delta \end{bmatrix} \begin{bmatrix} \ddot{\theta}_1 \\ \ddot{\theta}_2 \end{bmatrix} + \begin{bmatrix} -\beta s_2 \dot{\theta}_2 & -\beta s_2 (\dot{\theta}_1 + \dot{\theta}_2) \\ \beta s_2 \dot{\theta}_1 & 0 \end{bmatrix} \begin{bmatrix} \dot{\theta}_1 \\ \dot{\theta}_2 \end{bmatrix} + \begin{bmatrix} -\varphi s_{12} - \upsilon s_1 & \varphi c_{12} + \upsilon c_1 \\ -\varphi s_{12} & \varphi c_{12} \end{bmatrix} \begin{bmatrix} \ddot{x}_s \\ \ddot{y}_s \end{bmatrix} = \begin{bmatrix} \tau_1 \\ \tau_2 \end{bmatrix} \quad (3)$$

where

$$\alpha = I_{z1} + I_{z2} + m_1 r_1^2 + m_2 (l_1^2 + r_2^2)$$

$$\beta = m_1 l_1 r_2$$

$$\delta = I_{z2} + m_2 r_2^2$$

$$\varphi = m_2 r_2$$

$$\upsilon = m_1 r_1 + m_2 l_1 \quad (4)$$

The rigid body dynamics can be rewritten in the concise form

$$I(\theta)\ddot{\theta} + H(\theta, \dot{\theta})\dot{\theta} + N(\theta)\ddot{X}_s = \tau$$

$$\tau^I + \tau^H + \tau^N = \tau \quad (5)$$

Thus, the torque can be expressed as the sum of three components that depend on three system-dependent matrices. I is the matrix of inertia, H represents the Coriolis-centrifugal components of the torques, and N is the matrix that transformed the acceleration of the moving shoulder into joint torque components. Equations (3)–(5) show how the inertial matrix depends on the kinematics.

2.3 The Body Type. The subject body type or "somatotype" as originally defined by Sheldon [64] and subsequently revised by Carter [65,66] described the morphology of the subject's body. The shape of the body can be characterized using three main somatotypes: (1) the athletic body type with wide shoulders and thin waist, referred to as mesomorphic, (2) the soft and round body type with the ventral part larger than the waist, defined as endomorphic, and (3) the slender body type usually tall with thin shoulders, called ectomorphic. The physical structure of a subject is the combination of size (weight and height) and somatotype.

Most models of BSPs relate their estimates to the weight and height of the subject [23,38], and often either one is used to normalize the kinetic variables across subjects. However, individuals with the same height and weight but with different body types have dissimilar arm geometry. This causes a different spatial distribution of the arm mass, thus producing a different moment of inertia about the joints. If the method considered to estimate the BSPs is particularly sensitive to the somatotype of the subject, normalizing the kinetic variables with respect to weight and height alone might be deceiving. We divided our subjects into the three somatotype groups: mesomorphic, endomorphic, and ectomorphic, consisting of four, five, and four subjects, respectively. The somatotype appeared as a factor in the statistical analysis of the inertial parameter estimation and the kinetic variables.

2.4 Data Processing. A Lilliefors test [67] indicated that BSP populations, calculated with each estimation method, could be considered normally distributed across subjects. We first performed a one-way analysis of variance (ANOVA) and pairwise one-way ANOVAs to compare BSP populations across estimation methods and across subjects; we considered one BSP at a time (i.e., M, CM, or IM) for each section of the arm (i.e., hand, forearm, and upper arm). To analyze the combined influence of both BSP estimation methods and subjects' body type, a two-way ANOVA was also carried out.

For both elbow and shoulder, we evaluated two kinetic variables for each across-subject population of reaches: The normalized joint torque peak and the normalized root mean square (NRMS) of the joint torque.

The absolute values of torque peaks occurring before the maximum velocity of the reach were normalized to the weight of the subject in order to limit the effect of the subject's size on the distribution of joint torque peaks. Absolute values of shoulder and elbow torque peaks were considered to account for the fact that when reaching, the shoulder angular displacement θ_1 progressively increases, while the elbow angular displacement θ_2 decreases (Fig. 2(*b*)), which results in angular acceleration and torque profiles of opposite signs for the two joints.

The NRMS of torques for the whole movement was defined as follows [5,47]:

$$(\mathrm{NRMS}_i^j)_k = \frac{\sqrt{1/T \int_0^T (\tau_i^j(t))_k^2 dt}}{1/N \sum_{j=1}^{N} \left(\max(\tau_i^j(t)) - \min(\tau_i^j(t))\right)^{0<t<T}_{\text{all } k}} \quad (6)$$

where $j \in N | j = 1, \ldots, 9$ identified each BSP estimation method, T was the total duration of the reaching movement, and $(\tau_i^j(t))_k$ was the time-varying torque signal of the ith joint (i.e., $i=1$ for shoulder and $i=2$ for the elbow) calculated during the kth reach using the jth estimation method. The expression $\max(\tau_i^j(t))$ represents the maximum torque within the interval $0<t<T$ for all the k trials calculated with the jth method.

The rms of a joint torque is a parameter that expresses with a single number the modulation of torque throughout the reaching trajectory. A high rms of torque means a higher average absolute value of torque during the movement. Normalizing the rms of torque with respect to the subject weight, in the same fashion as the torque peak, would not capture the difference between torque profiles with similar rms but different amplitude range. A peak-to-peak normalization (Eq. (6)) highlights the difference between torque profile shapes: For a given rms, torque profiles that span a wider range have a lower NRMS. This allows for a fairer intra-subject comparison of torque profiles across methods; as for a given subject, differences in torque profile shapes across methods that do not result in different rms of torque are captured by the peak-to-peak normalization, but would be lost with a normalization by subject weight. Nine distributions of each kinetic variable, corresponding to the nine BSP estimation methods, were calculated across subjects. A grand distribution of kinematic variables was also obtained by considering the whole population of reaching movements among all subjects.

The experiment was designed to restrict the movement of each subject's arm to the same trajectory in the joint angle space. The maximum angular acceleration for each joint was reached approximately at the same angular configuration across subjects. Torque peak for each joint would also occur in the proximity of the angle of maximum acceleration (Fig. 8). The inertial matrix at the angle of torque peak would be only dependent on the subject's BSPs (cf. Eq. (3)). Assuming each BSP estimation method hypothetically independent of the subject's body type, the average of each normalized torque peak distribution would be dependent on the method used to estimate the BSPs (method effect) while the dispersion would only depend on the variability of kinematic variables at the configuration of torque peak, across subjects, and across trials (subject effect). Since the effect of the subject size on the distribution of joint torque peaks is minimized by the normalization, a change in the dispersion of torque peak distributions across methods indicates that an interaction between the method and the body type of the subjects accounts for the additional variance (interaction effect). Hence, we expect the variance of the normalized torque peak to depend on the method, the subject kinematic variability, and an interaction mostly related to the subject somatotype.

Similarly, the variance of the distribution of NRMS of joint torques was affected by the subject effect, the method effect, and the effect of an interaction between factors. However, the inertial

matrix changed as a function of the joint angle (Eq. (3)), resulting in an additional source of interaction between the subjects' kinematic variability and the variability across BSP estimation methods.

To determine the extent to which each effect affected the computation of the inertial parameters and the kinetics, we used the statistic η^2:

$$(\eta^2_{\text{group}_{\text{variable}}})_{\text{effect}} = \frac{SS_{\text{group}_{\text{effect}}}}{SS_{\text{group}_{\text{total}}}} \tag{7}$$

For each joint and each kinetic variable, $SS_{\text{ALL}_{\text{effect}}}$ was the sum of the squared differences between the total mean of the population μ_{ALL} (all movements, all methods, and all subjects) and the means of the considered kinetic variable population given either the method (all movements, one method, and all subjects), the subject (all movements, all methods, and one subject), or the interaction between subjects and methods (all movements, one method, and one subject), namely,

$$SS_{\text{ALL}_{\text{method}}} = \sum_{\text{all methods}} (\overline{(x_{\text{all subjects}})_{\text{method}}} - \mu_{\text{ALL}})^2$$

$$SS_{\text{ALL}_{\text{subject}}} = \sum_{\text{all subjects}} (\overline{(x_{\text{all methods}})_{\text{subject}}} - \mu_{\text{ALL}})^2$$

$$SS_{\text{ALL}_{\text{interaction}}} = \sum_{\text{all subjects}} \left(\sum_{\text{all methods}} (\overline{(x_{\text{subject}})_{\text{method}}} - \mu_{\text{ALL}})^2 \right) \tag{8}$$

$SS_{\text{ALL}_{\text{total}}}$ was the total variance of the kinetic variable across all subjects and all methods.

After analyzing the set of kinetic variable distributions obtained with all nine methods, we restricted our investigation to the method modeling the hand in the extended position, namely, McConville, Zatsiorsky (2002), water immersion, Zatsiorsky (1983), and de Leva. Equation (8) was modified to account for only the "hand extended" (HE) methods:

$$SS_{\text{HE}_{\text{method}}} = \sum_{\text{HE methods}} (\overline{(x_{\text{all subjects}})_{\text{method}}} - \mu_{\text{HE}})^2$$

$$SS_{\text{HE}_{\text{subject}}} = \sum_{\text{all subjects}} (\overline{(x_{\text{HE methods}})_{\text{subject}}} - \mu_{\text{HE}})^2$$

$$SS_{\text{HE}_{\text{interaction}}} = \sum_{\text{all subjects}} \left(\sum_{\text{HE methods}} (\overline{(x_{\text{subject}})_{\text{method}}} - \mu_{\text{HE}})^2 \right) \tag{9}$$

where μ_{HE} was the average of the considered kinetic variable distribution, across all subjects, and across all hand extended methods.

We also performed a pairwise comparison between methods to determine whether any two methods would produce comparable kinetic variables as well as whether any differences existed among different groups of distributions. Equations (8) and (9) showed that an interaction effect was proved to be statistically significant; therefore, a pairwise t-test or Tukey's honestly significant difference criterion could not be applied [68]. For each of the 36 possible combinations, Eq. (8) was modified by restricting the calculation of $SS_{\text{group}_{\text{effect}}}$ to the two methods considered pairwise, where μ_{pw} was the average of the distribution generated by all the subjects and two methods:

$$SS_{\text{pw}_{\text{method}}} = \sum_{\text{two methods}} (\overline{(x_{\text{all subjects}})_{\text{method}}} - \mu_{\text{pw}})^2$$

$$SS_{\text{pw}_{\text{subject}}} = \sum_{\text{all subjects}} (\overline{(x_{\text{two methods}})_{\text{subject}}} - \mu_{\text{pw}})^2$$

$$SS_{\text{pw}_{\text{interaction}}} = \sum_{\text{all subjects}} \left(\sum_{\text{two methods}} (\overline{(x_{\text{subject}})_{\text{method}}} - \mu_{\text{pw}})^2 \right) \tag{10}$$

Equation (7) was adapted to the pairwise comparison as well:

$$(\eta^2_{\text{pw}_{\text{variable}}})^{\text{joint}}_{\text{effect}} = \frac{SS^{\text{joint}}_{\text{pw}_{\text{effect}}}}{SS^{\text{joint}}_{\text{pw}_{\text{total}}}} \tag{11}$$

where $(\eta^2_{\text{pw}_{\text{variable}}})^{\text{joint}}_{\text{effect}}$ is obtained for each variable as the ratio of the SS_{effect} between the two considered distributions and SS_{total} within the union of those distributions. The effect size η^2 quantifies what percentage of the variance of a statistical population can be explained from the variance of the factors from which the population depends. According to the theory of measure, the variance of a variable is the squared standard uncertainty to be attributed to its mean. When a phenomenon can be described through a linear model, it is possible to analytically correlate the uncertainties of the inputs with those of the outputs through an error propagation analysis. Therefore, the variance of the population of kinetic variables can be compared with the standard uncertainty calculated from an error propagation analysis, considering the variance of the populations of BSPs and kinematics as the squared standard uncertainties of their respective means. In general, the squared combined standard uncertainty of $y=f(x_h)$, where $h \in N|h=1,\ldots,n$, is given by [69]

$$u_c^2(y) = \sum_{h=1}^{n} \left(\frac{\partial f}{\partial x_h} \right)^2 u^2(x_h) \tag{12}$$

where $u^2(x_h)$ is the squared uncertainty (i.e., the variance) of variable x_h.

Our data set (Fig. 8(*d*)) supports the results reported by Bortolami et al. [3,4] on baseline reaching movements, which have shown that the net contribution to the total joint torques τ of the terms dependent on the joint angular velocity (τ^H) and on the linear acceleration of the shoulder (τ^N) is at least one order of magnitude smaller than the contribution of the term τ^I, which depends on the segments' inertia. Therefore, in this specific case, the terms including H and N in Eq. (5) can be neglected when applying Eq. (12) (see Appendix):

$$u_c^2(\tau) = \ddot{\theta}^2 \cdot u^2(I) + I^2 \cdot u^2(\ddot{\theta}) \tag{13}$$

It is important to note that all three terms in Eq. (5) were used in the actual calculation of joint torques. The aforementioned simplification was used only for the analysis of uncertainty expressed in Eq. (13), in which joint angular accelerations were nonetheless calculated with a moving shoulder model.

3 Results

We modeled the arm as a two-link planar system with a floating base (shoulder). For each subject, a 95% confidence dispersion ellipsis of the shoulder centroid position is presented in Fig. 3(*a*). The movement of the finger tip and the centroid of shoulder and elbow along the vertical axis (*Z*, Fig. 2, following the right hand rule) was at least an order of magnitude smaller than the hand movement trajectory along the *Y* axis (Fig. 3(*a*)). The reaching displacement was $Y_{\text{finger}}=0.234\pm0.039$ m, while for the rms along the vertical axis, we obtained $Z_{\text{finger}}=0.015\pm0.004$ m, $Z_{\text{elbow}}=0.015\pm0.007$ m, and $Z_{\text{shoulder}}=0.005\pm0.002$ m, respectively; therefore, the adoption of a planar arm model movement was justified.

Although the experimental setup was designed to achieve a consistent and comparable angular trajectory of the joints' across subjects, kinematics variability was important, especially when considering the elbow peak acceleration (Fig. 3(*b*)). A summary of the total acceleration distribution (all movements and all subjects) is depicted in the first two panels of Fig. 3(*a*). Notice that the rms

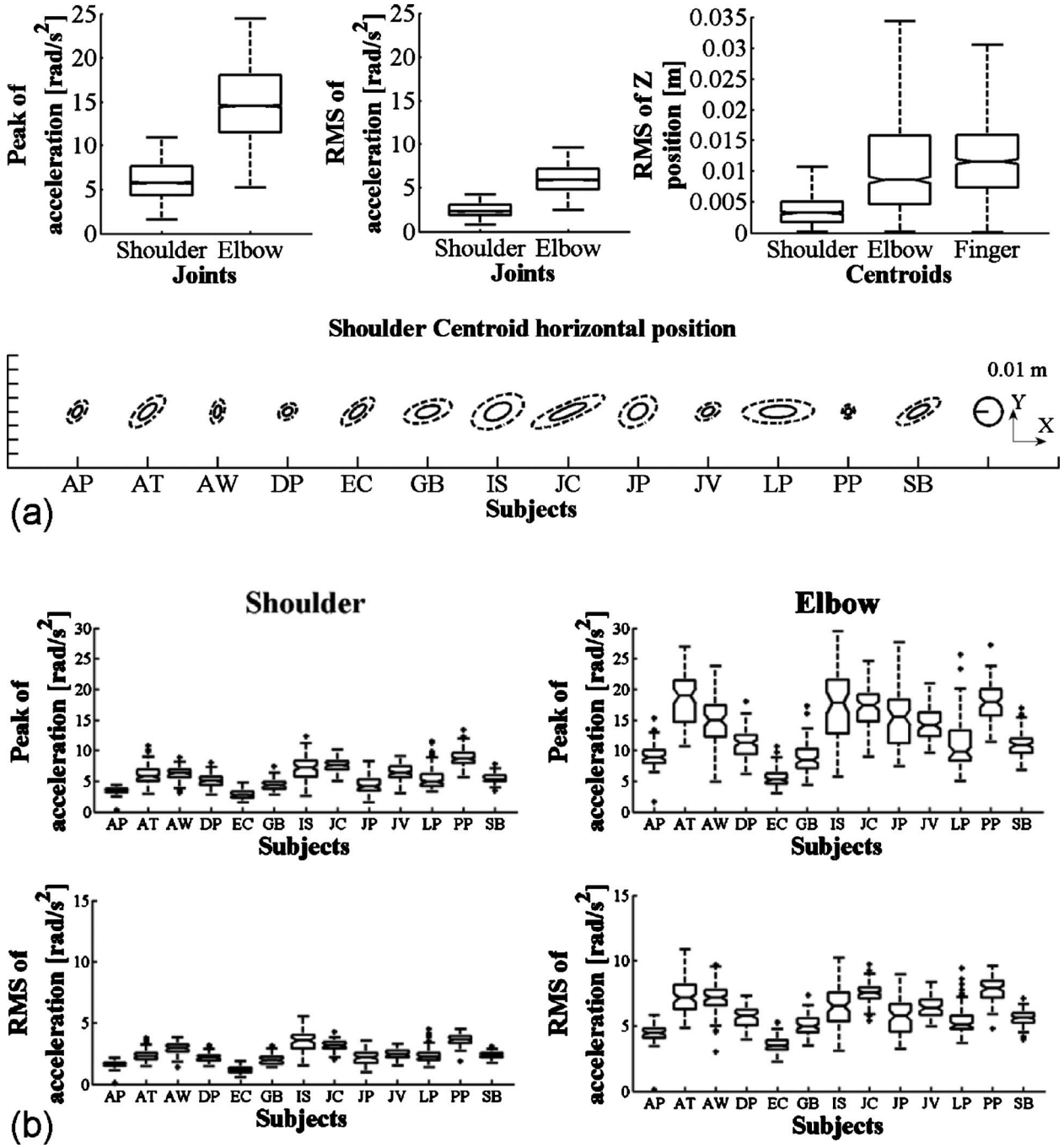

Fig. 3 (*a*) **Distributions of the kinematic variability for the arm reaching task. In the first row, the peak and rms of joint angular accelerations are represented along with the rms of the length of reach and the displacement of the finger tip, elbow centroid, and shoulder centroid along the vertical axis. The second row depicts the dispersion ellipses of the shoulder centroid on the plane of movement across subjects. Solid line represents one standard deviation and dashed line two standard deviations, enclosing 95% probability.** (*b*) **Quartile distribution of peak and rms of acceleration for each subject.**

of elbow angular acceleration is indeed much higher than that measured at the shoulder, $\ddot{\theta}_{\mathrm{rms}_{\mathrm{elbow}}}=6.0\pm1.6$ rad/s^2 versus $\ddot{\theta}_{\mathrm{rms}_{\mathrm{shoulder}}}=2.4\pm0.8$ rad/s^2, and so is the absolute value of the acceleration peak: $\ddot{\theta}_{\mathrm{peak}_{\mathrm{elbow}}}=13.3\pm5.2$ rad/s^2 versus $\ddot{\theta}_{\mathrm{peak}_{\mathrm{shoulder}}}=5.6\pm2.0$ rad/s^2.

3.1 Segment Parameters. Commentary to Fig. 4: A one-way ANOVA revealed that the BSP population computed with at least one method was significantly different from the others (maximum result $\mathrm{IM}_{\mathrm{forearm}}|F_{(8,108)}=2.72$, $p<0.009$). The pairwise comparisons showed that the different estimation models led to different results for each individual BSP.

The hand BSPs had the greatest variability across different methods. Estimations of the hand BSPs were quite diverse even across regression methods that assumed the same shape for the hand. The mean hand masses were $(\mathrm{M}_{\mathrm{hand}})_{\mathrm{ALL}}=0.53\pm0.08$ kg and $(\mathrm{M}_{\mathrm{hand}})_{\mathrm{HE}}=0.48\pm0.08$ kg across all nine methods and the hand extended methods, respectively (Fig. 4(*a*)). The estimated hand masses obtained by the methods of Hanavan, McConville, and Clauser were statistically different from most of the other methods.

The estimation of the hand CM was compatible within three

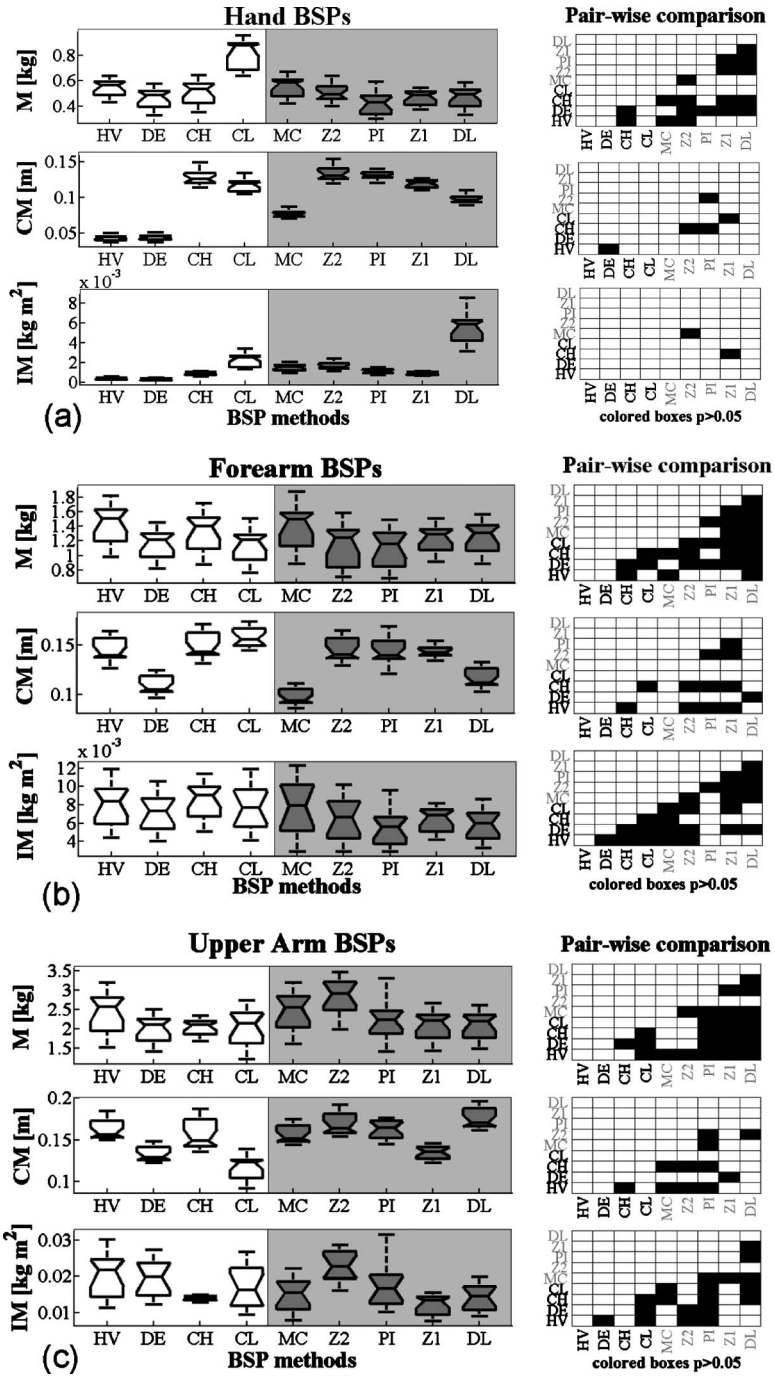

Fig. 4 Quartile distribution of body segment parameters. The figure shows the populations of mass (M), center of mass location (CM) with respect to the proximal end, and inertial moment about the proximal end (IM) of each section as a function of the estimation method. The right hand panel indicates the pairwise compatibility of the distributions across methods: Hanavan (HV), Dempster (DE), Chandler (CH), Clauser (CL), McConville (MC), Zatsiorsky and Seluyanov (1983) (Z1), water immersion (PI), Zatsiorsky (2002) (Z2), and de Leva (DL). Boxes with gray background correspond to "hand extended" methods. (*a*) Hand BSPs, (*b*) forearm BSPs, and (*c*) upper-arm BSPs.

distinct groups of methods: Hanavan–Dempster (CM_{hand} $=0.045\pm0.004$ m, $F_{(1,24)}=0.13$, $p=0.72$), which modeled the hand as sphere/fist-shaped; Chandler–Zatsiorsky (2002)-water immersion method ($CM_{hand}=0.128\pm0.010$ m, $F_{(2,36)}=1.84$, $p=0.17$), which modeled the hand as relaxed (Chandler) or fully extended; and Clauser–Zatsiorsky (1983), which assumed a slightly flexed (Clauser) or fully extended hand ($CM_{hand}=0.117\pm0.008$ m, $F_{(1,24)}=0.92$, $p=0.35$). Both McConville ($CM_{hand}=0.076\pm0.004$ m) and de Leva ($CM_{hand}=0.097\pm0.006$ m) gave statistically different estimations to all

the other methods and both modeled the hand as extended.

IM of the hand was the parameter with the largest variance across methods. With the exception of the pair of methods by McConville and Zatsiorsky (2002) ($IM_{hand}=0.0016\pm0.0003$ kg m^2, $F_{(1,24)}=1.61$, $p=0.22$) and Chandler–Zatsiorsky (1983) ($IM_{hand}=0.0009\pm0.0002$ kg m^2, $F_{(1,24)}=0.04$, $p=0.84$), all methods produced statistically different hand IM estimations: $(IM_{hand})_{ALL}=0.0016\pm0.0004$ kg m^2 and $(IM_{hand})_{HE}=0.0021\pm0.0005$ kg m^2 (Fig. 4(*a*)). None of the methods were pairwise compatible for all the three hand BSPs (M, CM, and IM).

Methods could be arranged into two main groups according to their estimated forearm mass: Hanavan–Chandler–McConville estimated a mean forearm mass of $M_{forearm}=1.377\pm0.277$ kg ($F_{(2,36)}=0.47$, $p=0.63$), while all the remaining methods estimated $M_{forearm}=1.16\pm0.23$ kg ($F_{(5,72)}=0.91$, $p=0.48$). A different grouping would consider Hanavan as an overestimating outlier of the forearm mass ($M_{forearm}=1.423\pm0.263$ kg), the water immersion method as an underestimating outlier ($M_{forearm}=1.095\pm0.265$ kg), and all the other methods compatible to each other ($M_{forearm}=1.228\pm0.239$ kg, $F_{(6,84)}=2.17$, $p=0.054$). The forearm mass distributions were generally not symmetrical, presenting a consistent skewness toward higher masses independent of the methods used for the estimation (Fig. 4(*b*)).

The pair of methods by Dempster and de Leva gave a mean forearm CM position value of $CM_{forearm}=0.113\pm0.009$ m ($F_{(1,24)}=3.54$, $p=0.072$); Clauser and McConville gave $CM_{forearm}=0.157\pm0.010$ m and 0.098 ± 0.008 m, respectively, while all the other method estimates were comparable, $CM_{forearm}=0.146\pm0.011$ m ($F_{(4,60)}=0.61$, $p=0.66$). The populations of forearm CM were all skewed with means toward lower values. Almost all methods were pairwise compatible and had symmetrically distributed estimates of forearm IM with means around $IM_{forearm}=0.0070\pm0.0022$ kg m^2.

Groups that gave compatible results for all three forearm BSPs where Zatsiorsky (2002)-water immersion-Zatsiorsky (1983) ($M|F_{(2,36)}=1.11$, $p=0.34$; $CM|F_{(2,36)}=0.16$, $p=0.85$; $IM|F_{(2,36)}=0.83$, $p=0.40$), Chandler–Clauser ($M|F_{(1,24)}=3.5$, $p=0.073$; $CM|F_{(1,24)}=3.04$, $p=0.094$; $IM|F_{(1,24)}=0.63$, $p=0.43$), Chandler–Hanavan ($M|F_{(1,24)}=1.02$, $p=0.32$; $CM|F_{(1,24)}=0.65$, $p=0.43$; $IM|F_{(1,24)}=0.21$, $p=0.65$), and Dempster–de Leva ($M|F_{(1,24)}=1.31$, $p=0.26$; $CM|F_{(1,24)}=3.54$, $p=0.072$; $IM|F_{(1,24)}=2.94$, $p=0.1$) (Fig. 4(*b*)).

The estimation of the upper-arm BSPs was quite consistent across methods. Two compatible groups estimate similar upper-arm mass: Hanavan–Zatsiorsky (2002) estimated $M_{upper\_arm}=2.61\pm0.50$ kg ($F_{(1,24)}=1.31$, $p=0.26$) and all the other methods estimated $M_{upper\_arm}=2.12\pm0.40$ kg ($F_{(6,84)}=1.82$, $p=0.10$).

The estimation of upper-arm CM was not homogeneous. While de Leva and Clauser provided the higher and the lower estimates ($CM_{upper\_arm}=0.175\pm0.013$ m and $CM_{upper\_arm}=0.117\pm0.016$ m, respectively), all the other methods could be divided into two groups: Dempster–Zatsiorsky (1983) provided $CM_{upper\_arm}=0.133\pm0.009$ m ($F_{(1,24)}=0.31$, $p=0.58$) while all the remaining methods estimated $CM_{upper\_arm}=0.162\pm0.014$ m ($F_{(4,48)}=1.8$, $p=0.16$).

The populations of upper-arm IM had comparable distributions with the exception of the distribution produced by Chandler, which had a significantly lower variance. The variability of forearm and upper-arm estimated parameters across methods was significant ($\pm33\%$), despite the fact that, unlike the hand, these cannot assume multiple configurations.

Commentary to Fig. 5: As we noted above, as a first approximation, the contribution of terms H and N to the total joint torques could be neglected; therefore, we limited the statistical analysis of inertial parameters to α, β, and δ, which appeared in matrix I. The distributions of the three parameters were similar across methods, but their variability was much higher compared with the single BSPs (M, CM, and IM). This could be attributed to the interdependency among BSPs: A change in any one BSP results in changes to the other two, leading to a variation in α, β, and δ larger than the variation on any single BSP. Methods could be grouped into two sets with similar distributions of all the three inertial matrix parameters: Hanavan, Dempster, Clauser, McConville, and de Leva estimated $\alpha=0.362\pm0.104$ kg m^2 ($F_{(4,60)}=1.42$, $p=0.23$), $\beta=0.119\pm0.034$ kg m^2 ($F_{(4,60)}=1.27$, $p=0.29$), and $\delta=0.118\pm0.034$ kg m^2 ($F_{(4,60)}=1.39$, $p=0.25$), while Chandler, the two methods of Zatsiorsky, and water immersion produced $\alpha=0.302\pm0.087$ kg m^2 ($F_{(3,48)}=0.56$, $p=0.64$), $\beta=0.090\pm0.028$ kg m^2 ($F_{(3,48)}=0.61$, $p=0.61$), and $\delta=0.077\pm0.024$ kg m^2 ($F_{(3,48)}=0.83$, $p=0.48$) (Fig. 5).

A two-way ANOVA, with the method and the somatotype as fixed factors and the subject as a random factor, showed what percentage of the variance within inertial parameter distributions could be attributed to differences in somatotype, which was rather homogeneous across the three inertial matrix parameters ($\eta^2_{\alpha_{somatotype}}=\eta^2_{\beta_{somatotype}}=\eta^2_{\delta_{somatotype}}=14\%$) and to methods, which was higher ($\eta^2_{\alpha_{method}}=15\%$, $\eta^2_{\beta_{method}}=23\%$ $\eta^2_{\delta_{method}}=36\%$). The remaining variance had to be explained by the variability of anthropometric features across the subjects population.

3.2 Joint Torques. Commentary to Fig. 6: Shoulder and elbow joint kinetics distributions were calculated from the distributions of estimated BSPs (Eq. (5)). Figure 6(*a*) shows the distribution of normalized torque peaks for both shoulder and elbow joints as a function of the method across subjects and as a function of the subject across methods. The dispersion of normalized torque peak means across methods was higher for the elbow than for the shoulder, even across methods representing the hand in the same configuration. In fact, the water immersion and McClauser methods (Fig. 6(*a*) top right panel), both of which assumed the hand as "extended," produced the largest difference between the means of the elbow normalized torque peak distributions. The variance of normalized torque peak populations across subjects was uniform ($(\eta^2_{torque\_peak})_{interaction}$ was small), suggesting that normalizing the torque peaks with the subject weight limited the effect of the subjects' body type on the estimation of kinetic variables.

The method effect $(\eta^2_{torque\_peak})_{method}$ on the normalized torque peak distributions was more evident at the elbow ($(\eta^2_{ALL_{torque\_peak}})^{elbow}_{method}=29\%$, $(\eta^2_{HE_{torque\_peak}})^{elbow}_{method}=31\%$) than at the shoulder ($(\eta^2_{ALL_{torque\_peak}})^{shoulder}_{method}=5\%$, $(\eta^2_{HE_{torque\_peak}})^{shoulder}_{method}=6\%$). For elbow and shoulder, respectively, $(\eta^2_{torque\_peak})_{subject}$ were 44% and 48% for all the methods and 43% and 49% for the hand extended methods. Statistical errors coming from sources independent of subjects, methods, and their interactions made up for ($(\eta^2_{ALL_{torque\_peak}})^{elbow}_{other\_source}=25\%$, $(\eta^2_{HE_{torque\_peak}})^{elbow}_{other\_source}=22\%$) and ($(\eta^2_{ALL_{torque\_peak}})^{shoulder}_{other\_source}=45\%$, $(\eta^2_{HE_{torque\_peak}})^{shoulder}_{other\_source}=43\%$) of the normalized torque peak variance at the elbow and shoulder, respectively.

Both shoulder and elbow normalized torque peak distributions across methods had many outliers and many observations clustered far from the mean (positive kurtosis). High kurtosis does not emerge in any of the distributions of NRMS for each subject (central panel of Fig. 6(*b*)).

NRMS distributions for both elbow and shoulder were more affected by the interaction effect than the distributions of normalized torque peaks (Fig. 6(*b*)). The variance of the distributions of NRMS of torque influenced by the subject effect was minimal: For the shoulder, we found that $(\eta^2_{ALL_{NRMS}})^{shoulder}_{subject}=8\%$ and

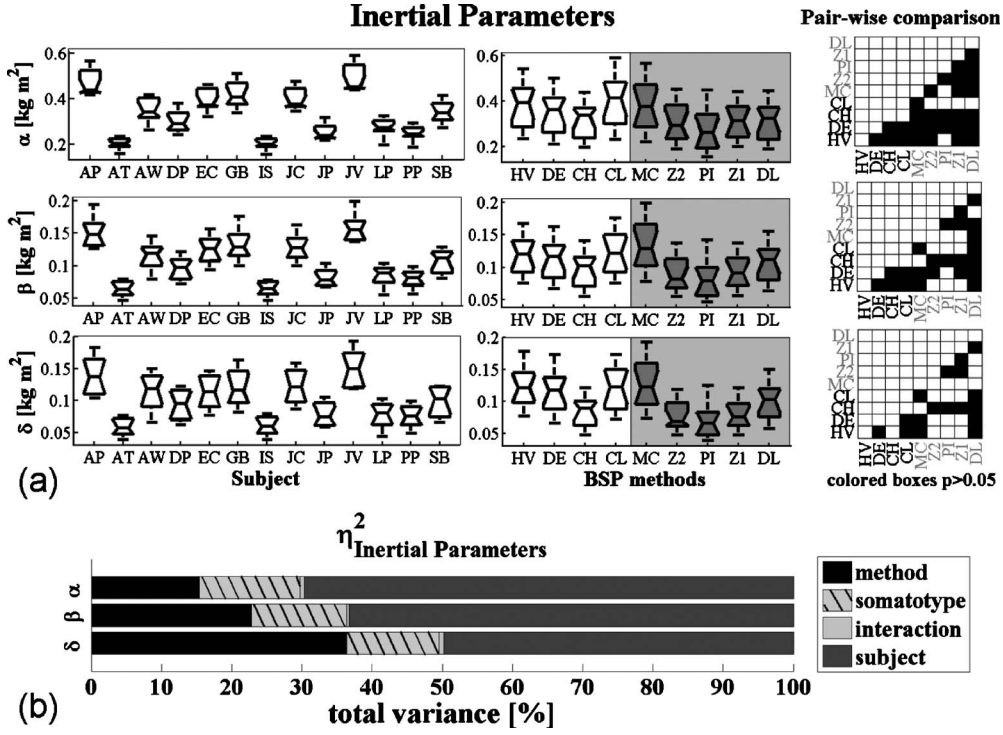

Fig. 5 (*a*) **Quartile distribution of inertial parameters α, β, and δ. The central panel shows the populations of parameters as a function of the estimation method. The left hand panel indicates the population of parameters for each subject across methods. The right hand panel indicates the pairwise compatibility of the distributions across methods. Gray background boxes correspond to "hand extended" methods.** (*b*) **Two-way ANOVA on the inertial parameters: variance accounted for when considering the subjects' somatotype as a factor. Subjects were divided in three groups: mesomorphs (4), endomorphs (5), and ectomorphs (4). For each of the nine methods, the influence of each factor was analyzed. The variance attributed neither to the method nor to the somatotype had to be attributed to the variability of anthropometric dimensions across subjects.**

$(\eta^2_{HE_{NRMS}})^{shoulder}_{subject}=14\%$, while for the elbow $(\eta^2_{ALL_{NRMS}})^{elbow}_{subject}=6\%$ and $(\eta^2_{HE_{NRMS}})^{elbow}_{subject}=7\%$. The method effect accounted for most of the variance, especially for the distributions of elbow kinetics: $(\eta^2_{ALL_{NRMS}})^{elbow}_{method}=84\%$ and $(\eta^2_{HE_{NRMS}})^{elbow}_{method}=85\%$, while for the shoulder, $(\eta^2_{ALL_{NRMS}})^{shoulder}_{method}=38\%$, $(\eta^2_{HE_{NRMS}})^{shoulder}_{method}=40\%$.

Interestingly, the effect of the interaction between method and subject had more influence on the distributions of torque NRMS at the shoulder than at the elbow: $(\eta^2_{ALL_{NRMS}})^{shoulder}_{interaction}=22\%$ and $(\eta^2_{HE_{NRMS}})^{shoulder}_{interaction}=17\%$, while $(\eta^2_{ALL_{NRMS}})^{elbow}_{interaction}=4\%$ and $(\eta^2_{HE_{NRMS}})^{elbow}_{interaction}=3\%$. The percentages of torque NRMS variance independent of subject, method, and interaction effects were close to 30% and 6% for the shoulder and elbow, respectively.

Commentary to Fig. 7: For each pair of estimating methods, the η^2 analysis of variance for the shoulder and elbow kinetic variables is shown. The variance of each pairwise combination was normalized with the total variance within the pairwise distribution (see Eq. (11)). The distributions within each pair combination of normalized torque peaks at the shoulder were mainly influenced by the subject effect and by statistical errors attributed to other sources, while the variability due to the interaction between method and subject effects was small across all pairwise combinations (Fig. 7(*a*)). On the other hand, a significant portion of the variance of the normalized torque peak at the elbow (up to 44%) was attributed to the method effect.

Across most of the pair combinations, the torque NRMS variance for both elbow and shoulder was influenced in a significant way by all three main effects (subject, method, and interaction). The influence of the subject was comparable for both joints while the method effect was more pronounced for the elbow torque NRMS. The influence of the method effect was more evident in the variance of both kinetic variables at the elbow than at the shoulder. In particular, among all methods modeling the hand in the extended configuration, we found the choice of BSP estimation method to be the principal source of variability in the computation of elbow torque NRMS. Moreover, almost all the pairwise comparisons involving the Zatsiorsky and water immersion methods demonstrated to be sensitive to the interaction effect.

The variance of the elbow torque peak distributions was the most affected by the method effect; therefore, we applied an analytical model to further analyze such findings. The elbow torque $\tau_2(t)$ is a function of time, and its variance $u^2(\tau_2)$ can be calculated at each instant from our data set. Using the theory of error propagation, we could compare the calculated torque variance $u^2(\tau_2)$ at a certain instant with the squared standard uncertainty of torque $u_c^2(\tau_2)$ calculated using Eq. (13). The squared standard uncertainty allowed us to understand the influence of kinematic variability and BSP variability on the final variance of the torque. Using Eqs. (13) and (3) we could write (see Appendix)

$$u_c^2(\tau_2) = \ddot{\theta}_1^2 \cdot u^2(I_{21}) + \ddot{\theta}_2^2 \cdot u^2(\delta) + I_{21}^2 \cdot u^2(\ddot{\theta}_1) + \delta^2 \cdot u^2(\ddot{\theta}_2) \tag{14}$$

where I_{21} and δ are, respectively, the element (2,1) and the element (2,2) of the matrix of inertia I (Eq. (5)). For each instant t_0, $u_c^2(\tau_2)$ is the squared standard uncertainty of the elbow joint torque at angular configuration $\theta(t_0)$, $u^2(I_{21})$ and $u^2(\delta)$ are the variances of the respective inertial parameters across all methods and all subjects, and $u^2(\ddot{\theta}_i)$ are the variances of the distributions of

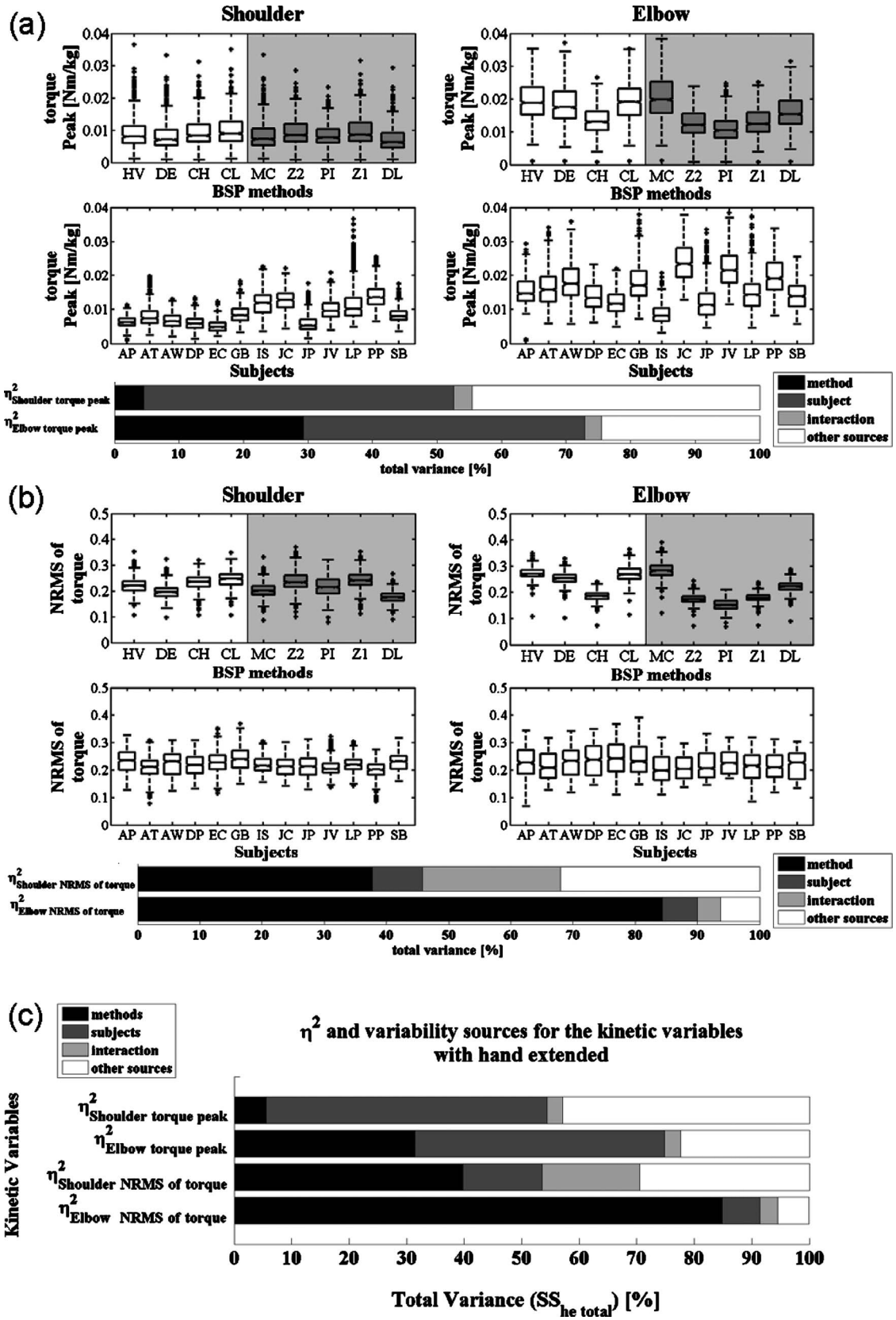

Fig. 6 Distributions of joint kinetic variables. Data relative to the shoulder and elbow kinetic variables are reported on the left and right panels, respectively. The top panels show the distribution of kinetic variables across subjects as a function of the estimation method. The central panels show the distribution of kinetic variables across subjects. The bottom bar plot illustrates the influence of different effects on the kinetic variable variance. Boxes with gray background correspond to "hand extended" methods. (*a*) Normalized torque peaks, (*b*) NRMS of torque, and (*c*) variance accounted for when using only hand extended methods.

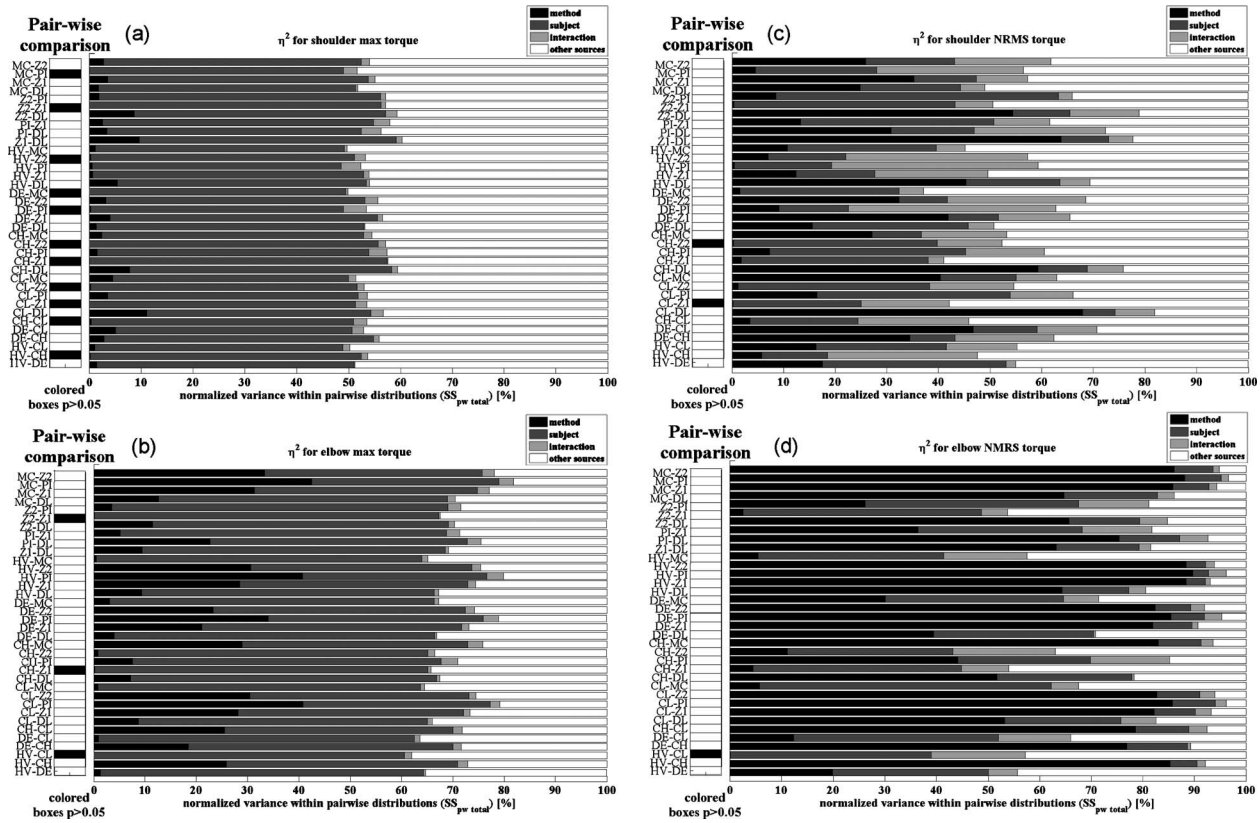

Fig. 7 Normalized η^2 analysis for each pairwise estimation method combination. The figure shows the contribution of method, subject, and interaction effect as well as other sources to the variance of the joint kinematic variables. The total variance of each method combination is indicated as a percentage of the total variance within the union of each pair of distributions. (*a*) Shoulder normalized torque peaks, (*b*) elbow normalized torque peaks, (*c*) shoulder NRMS of torque, and (*d*) elbow NRMS of torque.

joint angular accelerations across all methods and all subjects at angular configuration $\theta(t_0)$. For each instant, all the aforementioned components, as well as the means of $\ddot{\theta}_1(t)$ and $\ddot{\theta}_2(t)$, are shown in Figs. 8(*a*) and 8(*c*), respectively. The absolute value of the elbow torque reaches its peak around the same time as both joint accelerations (Fig. 8(*d*)). Around the same point in the trajectory, the inertial parameters δ and especially I_{21} have very low absolute values (Fig. 8(*c*)). The terms $\ddot{\theta}_1^2 \cdot u^2(I_{21})$ and especially $\ddot{\theta}_2^2 \cdot u^2(\delta)$ represent the major source of variance for the elbow torque peak, as can be seen in Fig. 8(*e*). The contribution of the other two terms $I_{21}^2 \cdot u^2(\ddot{\theta}_1)$ and $\delta^2 \cdot u^2(\ddot{\theta}_2)$ was negligible. Figure 8(*f*) shows a comparison of the variance of the elbow torque distribution estimated from the data across all subjects and methods (statistical method) and from Eq. (14) (analytical method). As expected, the two methods produce comparable results.

During the movement, I_{21} rises monotonically with the angle θ_2, and its estimation is progressively more dispersed across methods (Fig. 8(*c*)); therefore, the contribution of term $\ddot{\theta}_1^2 \cdot u^2(I_{21})$ becomes a more predominant source of variance during the second half of the trajectory, despite the fact that $\ddot{\theta}_1$ is lower than $\ddot{\theta}_2$.

4 Discussion and Conclusions

We quantified, statistically and analytically, the influence of different error sources and their interactions on the estimation of inverse dynamics during multijoint fast, nonballistic arm reaching movements.

We found that the variance of both normalized torque peaks and normalized torque rms at the shoulder and elbow joints was influenced by (a) the differences in BSPs introduced by different estimation methods (method effect), (b) the subject-dependent kinematic variability and limited repeatability across trials (subject effect), (c) the interaction between the BSP estimation method and the subjects' body type (interaction effect), and (d) other effects such as nonsystematic errors.

We showed that the method effect was the primary cause of uncertainty in the estimation of the normalized rms of joint torques. The variability of the normalized rms of torque at the elbow did not depend much on the change in shape of the hand during the reaching movement, but did depend strongly on the change of the components of the inertial matrix along the trajectory as a function of the angular configuration of the joints. In fact, for five methods representing the hand as extended, we obtained $((\eta^2_{\mathrm{HE}_{\mathrm{NRMS}}})^{\mathrm{elbow}}_{\mathrm{method}} = 85\%)$. The motor task that we analyzed required the subject to keep his or her hand extended throughout the movement. We found that the variability of the distribution of kinetic variables introduced by BSP estimation methods that modeled the hand as completely extended was comparable to the variability introduced by methods representing the hand in different configurations.

A reaching movement could be described with models as complex as having up to 13 DOFs and five links [70]. The nonperfect planarity of the movement could account for part of the variance not explained by method, subject, and interaction effects. This modeling error could have been reduced by adopting a model of the arm with a higher number of degrees of freedom. However, this would have added a considerable computational and theoretical burden, and further assumptions would have been required in order to calculate the kinetic variables. Models with more than two degrees of freedom are seldom used in the study of upper limb motor control due to the difficulty to establish a trade-off

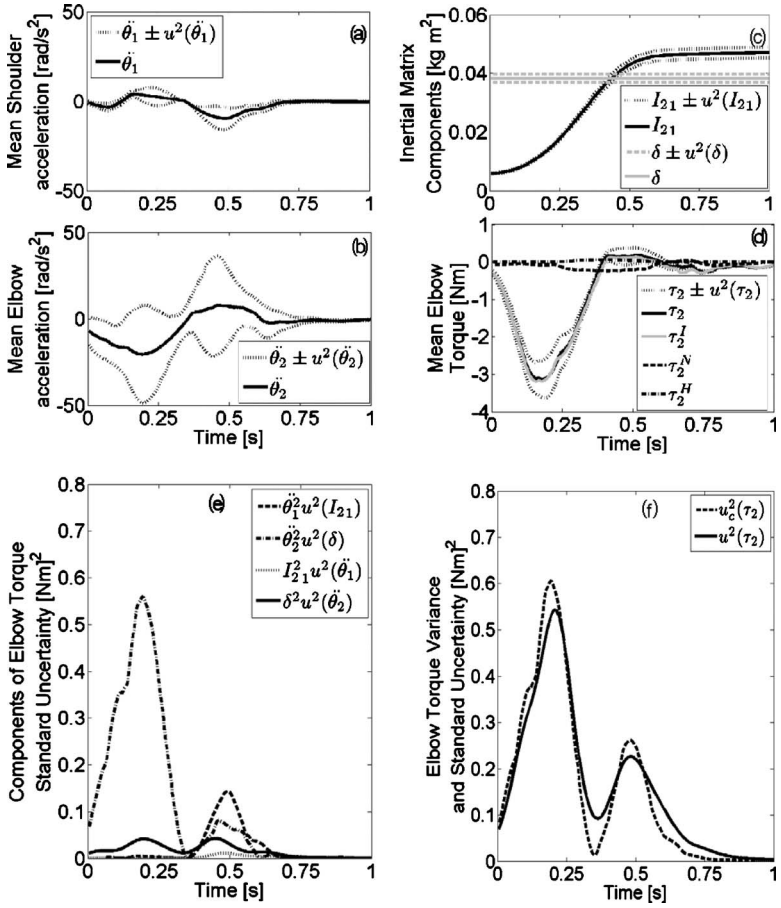

Fig. 8 Comparison between the variance of the non-normalized elbow torque estimated with Eq. (14) and the variance of the population of non-normalized elbow torques. (*a*) Mean of shoulder acceleration (solid) and associated variance (dotted). (*b*) Mean of elbow acceleration (solid) and associated variance (dotted). (*c*) Components of the inertial matrices I_{21} (black-solid) and I_{22} (i.e., δ gray-solid) and their associated variance (dotted). (*d*) Mean of non-normalized elbow torque τ_2 (black-solid) and associated variance (black-dotted). Here, we compared the different components of elbow torque τ_2 as they appear in Eq. (5). τ_2^H is proportional to the joint angular velocities (dashed-dotted), τ_2^N is proportional to the shoulder linear acceleration (dashed), and τ_2^I is proportional to the joint angular acceleration (gray-solid). Notice how τ_2^H and τ_2^N are close to zero and tend to cancel each other, confirming the assumption used to formulate Eq. (13). (*e*) Components of the variance of the non-normalized torque calculated using Eq. (14). The dashed-dotted line represents the component $\ddot{\theta}_2^2 \cdot u^2(\delta)$, while the dashed is $\ddot{\theta}_1^2 \cdot u^2(I_{21})$. The influence of the variability of the other components on the variance of the non-normalized elbow torque is negligible. (*f*) Comparison between the variance of τ_2 estimated point by point for all subjects and all data (solid) and $u_c^2(\tau_2)$ calculated from Eq. (14) (dashed). The maximum variance of the elbow torque aligns with the absolute torque peak, and it is mostly dependent on the variance component $\ddot{\theta}_2^2 \cdot u^2(\delta)$. Increased dependence on $\ddot{\theta}_1^2 \cdot u^2(I_{21})$ occurs toward the end of the movement where the $u^2(I_{21})$ increases concurringly with I_{21}.

between the complexity of the model and the assumptions required by the researcher to ensure model fit. The contribution of this paper is relevant for research concerned with upper limb motor control because it points out that even a simple model can show how the effect of BSP estimation methods and the interaction effect between the BSP methods and the subjects' body type are a considerable source of variance and could easily override modeling and kinematic errors.

Previous studies on the sensitivity of upper limb inverse dynamics to BSPs analyzed single-joint movements such as elbow flexion-extensions and, therefore, were not representative of generalized arm reaching tasks. Challis [41] reported a torque peak of about 6.5 N m for a single-joint elbow extension (throwing task). The value of the IM for the forearm and hand combined (δ in Eq. (3)) was not reported, and neither was the maximum acceleration, but the author used Chandler's [23] BSP estimation method. Since the task in Ref. [23] is a simple elbow extension and not a multijoint movement, α and β are not relevant as the dynamics equation reduces to simply $\tau_2 = \delta \cdot \ddot{\theta}_2$. An inverse dynamics analysis

that uses the average value of δ estimated with Chandler's method across our subject population, $\delta = 0.083 \pm 0.024$ kg m^2, results in an approximate maximum joint acceleration for the throwing task of 70 rad/s^2. Challis reported that a $\pm 5\%$ imposed variation of δ resulted in a variation of root mean square of joint torque of 4.1%. While a direct comparison of Challis' findings with our analysis of a bi-articular task would not be appropriate due to the significant effect of the shoulder rotation on the elbow torque (Eq. (5)), some observations can be made: Different BSP methods can produce differences of up to $\pm 50\%$ in the estimate of IM of the "hand +forearm" about the elbow, and the interdependency of BSPs increases the estimation variability in the calculation of δ (Fig. 5(*b*)). Also, from Eq. (14), we see that the effect of the variability of δ across estimation methods represents the most significant source of variability in the calculation of elbow joint torque, given the high acceleration typical of Challis' task. Therefore, Challis' sensitivity analysis, while numerically correct, is based on an underestimation of the variability of BSP estimations across methods.

Most of the inverse dynamics sensitivity analyses applied to multijoint movements found in literature focus on lower limb tasks. For lower limb analysis, the estimation of torque is reportedly sensitive to the variability of acceleration, and it has been hypothesized that the effect of uncertainties in the estimation of BSPs becomes noticeable when the acceleration is higher than a certain unspecified threshold [40,44,46,71,72]. Double-pendulum models are commonly used to represent reaching, gait, and posture. While unfettered arm reaches occur in a single continuous movement with no load at the end-point, a gait cycle is usually divided into a stance and a swing phase, which represent approximately 65% and 35% of the cycle, respectively [73]. Estimating the inverse dynamics of lower limbs during gait can benefit from two main characteristics of the movement that are absent in the study of arm dynamics: First, since during the stance phase both feet are in contact with the ground, the system can be modeled as a closed kinematic chain, and the limb acceleration is low when compared with the maximum. Second, at least one leg is always "loaded" with the weight of the subject and the ground reaction force can be used in the estimation of the joint torque at hip, knee, and ankle when using iterative algorithms such as Newton–Euler or bottom-up methods [5,45]. The highest variability in the estimation of kinetic variables is reported during the "swing" phase when the reaction force is not directly measurable [43,46,49].

The swing phase is the segment of gait most similar to the unfettered movement of a generic double-pendulum, which we used to model the arm reach, although the inertia of the limb, the effects of gravity, and the intrinsic nature of the movement are quite different. The kinematic variability during gait is a fundamental factor in the analysis of the kinetic error because variability in the kinematics is amplified by the big inertia of the limb (Eq. (14)). The maximum angular acceleration at the hip joint is approximately 38 rad/s^2 while just before heel strike, the maximum knee angular acceleration can reach 107 rad/s^2 [2]. These are much higher compared with the average maximum angular accelerations of approximately 5.6 rad/s^2 at the shoulder and 13.3 rad/s^2 at the elbow that we measured. Higher accelerations are prone to higher variance, and inertial parameters of the leg are three to five times larger than those of the arm: Average values for the inertial parameters of the lower limb are as follows: $\alpha = 1.72$ kg m^2, $\beta = 0.49$ kg m^2, and $\delta = 0.34$ kg m^2 [74] compared with $\alpha = 0.34$ kg m^2, $\beta = 0.11$ kg m^2, and $\delta = 0.10$ kg m^2 estimated by us for the upper limb across all methods and all subjects. Thus, the terms $I_{21}^2 \cdot u^2(\ddot{\theta}_1)$ and $\delta^2 \cdot u^2(\ddot{\theta}_2)$ of Eq. (14) are larger when analyzing leg movements compared with arm movements.

In both the leg and the arm, the segment with higher inertia is connected to the joint with slower average angular acceleration and vice versa; therefore, the variability in the estimation of the segments' inertia is generally inversely proportional to the variability of the measured acceleration of each joint. In our case, the variance of the acceleration was higher at the elbow than at the shoulder, while the inertial term α (Eq. (3)), used only to calculate the torque at the shoulder joint, had mean and variance 3–4 times higher than the parameters β and δ, the latter only used to calculate the elbow joint torque (Fig. 5). Hence, the normalized torque peak variance for both shoulder and elbow was comparable (Fig. 6(*a*)).

The parameters α, β, and δ were all comparable across some pairs of methods (see Fig. 5). While normalized torque peaks had comparable distributions across the same method pairs, that was not the case for the distributions of NRMS of torques. Joint accelerations and BSPs were required as input for the inverse dynamics model to calculate joint kinematic variables. The variance of the angular acceleration depended mostly on the limited repeatability of the subject, rather than on the inaccuracy of the measure of the kinetic variables. The method-specific regression equations used to estimate each BSP set could influence both the mean and the variance of the kinetic variable distributions across methods. Differences in the means could be induced by different model assumptions, such as the geometry of the hand, or different segmentation of the arm, while differences in variance arose from a combined effect between the method and the subject's body type. We adopted the NRMS of torque as a tool to analyze the differences across BSP estimation methods and across-subject body types. The central limit theorem states that the distribution of the sample average of these distributions approaches the normal distribution. Hence, the "mean of sample averages" is the most probable value of the actual kinetic variable. Therefore, assuming that the intrinsic variability of the task was the same across subjects, the most accurate BSP estimation method could be identified as that with the closest average to the mean of sample averages and minimal variance of NRMS of torques.

Among all nine methods analyzed, the one proposed by de Leva consistently estimated values of the kinetic variables closer to the average across all methods, still maintaining a small variance of NRMS. When restricting the analysis to the hand extended methods, the method proposed by Zatsiorsky (2002) produced the results closest to the average values, and it offers the most reliable set of regression equations for practical use.

Acknowledgment

This work was supported in part by NIH RO1 Grant No. AR48546-01. The authors would like to thank the Robotics Lab and Dr. Sandro Mussa-Ivaldi for their support. They are grateful to Dr. Eric Perreault and Dr. Yasin Dhaher for their useful suggestions and to the anonymous reviewers for their help to clarify several concepts of the paper.

Appendix

The results of the statistical analysis that we performed could be compared directly with a first-principle-based analysis of the uncertainty attributed to the kinematics of each trajectory point. As a first approximation, the shoulder translation and velocity-dependent terms of Eq. (5) could be neglected (as shown in Fig. 8(*d*)). Therefore, an analytical estimate of the joint torque uncertainty given the joint angles could be approximated as follows:

$$\tau(\ddot{\theta},I)|_{\hat{\theta}} \cong I \cdot \ddot{\theta}$$

$$\begin{bmatrix} \tau_1 \\ \tau_2 \end{bmatrix}_{\hat{\theta}} \cong \begin{bmatrix} I_{11} & I_{12} \\ I_{21} & I_{22} \end{bmatrix}_{\hat{\theta}} \begin{bmatrix} \ddot{\theta}_1 \\ \ddot{\theta}_2 \end{bmatrix}_{\hat{\theta}} = \begin{bmatrix} \alpha + 2\beta\cos(\hat{\theta}_2) & \delta + \beta\cos(\hat{\theta}_2) \\ \delta + \beta\cos(\hat{\theta}_2) & \delta \end{bmatrix} \times \begin{bmatrix} \ddot{\theta}_1 \\ \ddot{\theta}_2 \end{bmatrix}_{\hat{\theta}} \tag{A1}$$

Equation (A1) expresses the joint torques calculated in the neighborhood of the angular configuration $\hat{\theta}$. The combined standard uncertainty of the torque vector calculated at $\hat{\theta}$ is the square root of the combined standard variance as follows [69]:

$$u_c^2(\tau) = \sum_{h=1}^{N} \left(\frac{\partial f}{\partial x_h} \right)^2 \cdot u^2(x_h)$$

$$u_c^2(\tau) = \left(\frac{\partial \tau}{\partial I} \right)^2 \cdot u^2(I) + \left(\frac{\partial \tau}{\partial \ddot{\theta}} \right)^2 \cdot u^2(\ddot{\theta})$$

$$u_c^2(\tau) = \ddot{\theta}^2 \cdot u^2(I) + I^2 \cdot u^2(\ddot{\theta}) \tag{A2}$$

where f is any multivariate function (i.e., τ in Eq. (A1)) and x_h are the independent variables (i.e., I and $\ddot{\theta}$), each characterized by variance $u^2(x_h)$. By means of Eq. (A2) we can estimate the variance of the measured torque at any given angle attributed to all methods and all subjects and quantify the contribution of each component of the torque variance along the trajectory. Equation (14) was derived in the following way:

from Eq. (A1) we isolated τ_2 so that

$$\tau_2 = I_{21}(\theta_1) \cdot \ddot{\theta}_1 + I_{22} \cdot \ddot{\theta}_2$$

$$\tau_2 = I_{21}(\theta_1) \cdot \ddot{\theta}_1 + \delta \cdot \ddot{\theta}_2 \tag{A3}$$

From Eq. (A2) we calculated the combined standard variance:

$$u_c^2(\tau_2) = \left(\frac{\partial \tau_2}{\partial I_{21}} \right)^2 \cdot u^2(I_{21}) + \left(\frac{\partial \tau_2}{\partial \delta} \right)^2 \cdot u^2(\delta) + \left(\frac{\partial \tau_2}{\partial \ddot{\theta}_1} \right)^2 \cdot u^2(\ddot{\theta}_1) + \left(\frac{\partial \tau_2}{\partial \ddot{\theta}_2} \right)^2 \cdot u^2(\ddot{\theta}_2)$$

$$u_c^2(\tau_2) = \ddot{\theta}_1^2 \cdot u^2(I_{21}) + \ddot{\theta}_2^2 \cdot u^2(\delta) + I_{21}^2 \cdot u^2(\ddot{\theta}_1) + \delta^2 \cdot u^2(\ddot{\theta}_2) \tag{A4}$$

hence, obtaining Eq. (14).

References

[1] Hatze, H., 2000, "The Inverse Dynamics Problem of Neuromuscular Control," Biol. Cybern., **82**(2), pp. 133–141.

[2] Winter, D., 2005, *Biomechanics and Motor Control of Human Movement*, Wiley-Interscience, Toronto, ON, Canada.

[3] Bortolami, S., Pigeon, P., Dizio, P., and Lackner, J., 2008, "Kinetic Analysis of Arm Reaching Movements During Voluntary and Passive Rotation of the Torso," Exp. Brain Res., **187**(4), pp. 509–523.

[4] Bortolami, S., Pigeon, P., Dizio, P., and Lackner, J., 2008, "Dynamics Model for Analyzing Reaching Movements During Active and Passive Torso Rotation," Exp. Brain Res., **187**(4), pp. 525–534.

[5] Cahouët, V., Luc, M., and David, A., 2002, "Static Optimal Estimation of Joint Accelerations for Inverse Dynamics Problem Solution," J. Biomech., **35**(11), pp. 1507–1513.

[6] Holden, J. P., and Stanhope, S. J., 1998, "The Effect of Variation in Knee Center Location Estimates on Net Knee Joint Moments," Gait and Posture, **7**(1), pp. 1–6.

[7] Challis, J. H., and Kerwin, D. G., 1996, "Quantification of the Uncertainties in Resultant Joint Moments Computed in a Dynamic Activity," J. Sports Sci., **14**(3), pp. 219–231.

[8] Silva, M. P. T., and Ambrósio, J. A. C., 2004, "Sensitivity of the Results Produced by the Inverse Dynamic Analysis of a Human Stride to Perturbed Input Data," Gait and Posture, **19**(1), pp. 35–49.

[9] Dortmans, L., Jans, H., Sauren, A., and Huson, A., 1991, "Nonlinear Dynamic Behavior of the Human Knee Joint—Part I: Postmortem Frequency Domain Analyses," ASME J. Biomech. Eng., **113**(4), pp. 387–391.

[10] Charlton, I. W., Tate, P., Smyth, P., and Roren, L., 2004, "Repeatability of an Optimised Lower Body Model," Gait and Posture, **20**(2), pp. 213–221.

[11] Giakas, G., and Baltzopoulos, V., 1997, "Optimal Digital Filtering Requires a Different Cut-Off Frequency Strategy for the Determination of the Higher Derivatives," J. Biomech., **30**(8), pp. 851–855.

[12] McCaw, S. T., and DeVita, P., 1995, "Errors in Alignment of Center of Pressure and Foot Coordinates Affect Predicted Lower Extremity Torques," J. Biomech., **28**(8), pp. 985–988.

[13] Alexander, E. J., and Andriacchi, T. P., 2001, "Correcting for Deformation in Skin-Based Marker Systems," J. Biomech., **34**(3), pp. 355–361.

[14] Reinbolt, J. A., Schutte, J. F., Fregly, B. J., Koh, B. I., Haftka, R. T., George, A. D., and Mitchell, K. H., 2005, "Determination of Patient-Specific Multi-Joint Kinematic Models Through Two-Level Optimization," J. Biomech., **38**(3), pp. 621–626.

[15] Lu, T. W., and O'Connor, J. J., 1999, "Bone Position Estimation From Skin Marker Co-Ordinates Using Global Optimisation With Joint Constraints," J. Biomech., **32**(2), pp. 129–134.

[16] Chèze, L., Fregly, B. J., and Dimnet, J., 1995, "A Solidification Procedure to Facilitate Kinematic Analyses Based on Video System Data," J. Biomech., **28**(7), pp. 879–884.

[17] Kodek, T., and Munih, M., 2006, "An Identification Technique for Evaluating Body Segment Parameters in the Upper Extremity From Manipulator-Hand Contact Forces and Arm Kinematics," Clinical Biomechanics, **21**, pp. 710–716.

[18] Langenderfer, J. E., Laz, P. J., Petrella, A. J., and Rullkoetter, P. J., 2008, "An Efficient Probabilistic Methodology for Incorporating Uncertainty in Body Segment Parameters and Anatomical Landmarks in Joint Loadings Estimated From Inverse Dynamics," ASME J. Biomech. Eng., **130**(1), p. 014502.

[19] Kingma, I., Toussaint, H. M., Commissaris, D. A. C. M., Hoozemans, M. J. M., and Ober, M. J., 1995, "Optimizing the Determination of the Body Center of Mass," J. Biomech., **28**(9), pp. 1137–1142.

[20] Riemer, R., and Hsiao-Wecksler, E. T., 2009, "Improving Net Joint Torque Calculations Through a Two-Step Optimization Method for Estimating Body Segment Parameters," ASME J. Biomech. Eng., **131**, p. 011007.

[21] Clauser, C. E., McConville, J. T., and Young, J. W., 1969, "Weight, Volume, and Center of Mass of Segments of the Human Body," Wright-Patterson Air Force Base, Technical Report No. 69-70.

[22] Dempster, W. T., 1955, "Space Requirements of the Seated Operator. Geometrical, Kinematic, and Mechanical Aspects of the Body With Special Reference to the Limbs," Wright Air Development, Technical Report No. 55-159.

[23] Chandler, R. F., Clauser, C. E., and McConville, J. T., 1975, "Investigation of Inertial Properties of the Human Body," AMRL, Technical Report No. 74-137.

[24] Barter, J. T., 1957, "Estimation of the Mass of Body Segments," WADC, Technical Report No. 57-260.

[25] Hinrichs, R. N., 1985, "Regression Equations to Predict Segmental Moments of Inertia From Anthropometric Measurements: An Extension of the Data of Chandler Et Al. (1975)," J. Biomech., **18**(8), pp. 621–624.

[26] Hanavan, E. P. J., 1964, "A Mathematical Model of the Human Body," Wright-Patterson Air Force Base, Technical Report No. 64-102.

[27] Pavol, M. J., Owings, T. M., and Grabiner, M. D., 2002, "Body Segment Inertial Parameter Estimation for the General Population of Older Adults," J. Biomech., **35**(5), pp. 707–712.

[28] McConville, J. T., Churchill, T. D., Kaleps, I., Clauser, C. E., and Cuzzi, J., 1980, "Anthropometric Relationships of Body and Body Segment Moments of Inertia," Wright-Patterson Air Force Base, Technical Report No. 80-119.

[29] Jensen, R. K., 1978, "Estimation of Biomechanical Properties of Three Body Types Using a Photogrammetric Method," J. Biomech., **11**, pp. 349–358.

[30] Jensen, R. K., 1989, "Changes in Segment Inertia Proportions Between 4 and 20 Years," J. Biomech., **22**(6–7), pp. 529–536.

[31] Jensen, R. K., and Nassas, G., 1988, "Growth of Segment Principal Moments of Inertia Between Four and Twenty Years," Med. Sci. Sports Exercise, **20**(6), pp. 594–604.

[32] Ackland, T. R., Blanksby, B. A., and Bloomfield, J., 1988, "Inertial Characteristics of Adolescent Male Body Segments," J. Biomech., **21**(4), pp. 319–327.

[33] Drillis, R., and Contini, R., 1966, "Body Segment Parameters," New York University, Technical Report No. 1166.03.

[34] Piovesan, D., Bortolami, S. B., Debei, S., Pierobon, A., Chiovetto, E., Dizio, P., and Lackner, J. R., 2006, "Comparative Analysis of Methods for Estimating Arm Segment Parameters and Joint Torques," Neuroscience Meeting Planner, Society for Neuroscience, Atlanta, GA, 451.27, Online.

[35] Zatsiorsky, V., and Seluyanov, V., 1985, *Estimation of the Mass and Inertia Characteristics of the Human Body by Means of the Predictive Regression Equations*, D. A. Winter, R. W. Norman, R. P. Wells, K. C. Hayes, and A. E. Patla, eds., Human Kinetics, Champaign, IL, Vol. 5A–5B, pp. 233–239.

[36] Durkin, J. L., Dowling, J. J., and Andrews, D. M., 2002, "The Measurement of Body Segment Inertial Parameters Using Dual Energy X-Ray Absorptiometry," J. Biomech., **35**(12), pp. 1575–1580.

[37] Mungiole, M., and Martin, P. E., 1990, "Estimating Segment Inertial Properties: Comparison of Magnetic Resonance Imaging With Existing Methods," J. Biomech., **23**(10), pp. 1039–1046.

[38] Zatsiorsky, V., and Seluyanov, V., 1983, *The Mass and Inertia Characteristics of the Main Segments of the Human Body*, H. Matsui, and K. Kobayashi, ed., Human Kinetics, Champaign, IL, pp. 1152–1159.

[39] Zatsiorsky, V. M., 2002, "Kinetics of Human Motion," *Best Predictive Regression Equations for Estimating Inertial Properties of Body Segments in Males*, Human Kinetics, Champaign, IL, Appendix A2.8.
[40] Andrews, J. G., and Mish, S. P., 1996, "Methods for Investigating the Sensitivity of Joint Resultants to Body Segment Parameter Variations," J. Biomech., **29**(5), pp. 651–654.
[41] Challis, J. H., 1996, "Accuracy of Human Limb Moment of Inertia Estimations and Their Influence on Resultant Joint Moments," J. Appl. Biomech., **12**(4), pp. 517–530.
[42] Challis, J. H., and Kerwin, D. G., 1992, "Calculating Upper Limb Inertial Parameters," J. Sports Sci., **10**(3), pp. 275–284.
[43] Ganley, K. J., and Powers, C. M., 2004, "Determination of Lower Extremity Anthropometric Parameters Using Dual Energy X-Ray Absorptiometry: The Influence on Net Joint Moments During Gait," Clin. Biomech. (Bristol, Avon), **19**(1), pp. 50–56.
[44] Kingma, I., Toussaint, H. M., De Looze, M. P., and Van Dieen, J. H., 1996, "Segment Inertial Parameter Evaluation in Two Anthropometric Models by Application of a Dynamic Linked Segment Model," J. Biomech., **29**(5), pp. 693–704.
[45] Kuo, A. D., 1998, "A Least-Squares Estimation Approach to Improving the Precision of Inverse Dynamics Computations," ASME J. Biomech. Eng., **120**, pp. 148–159.
[46] Pearsall, D. J., and Costigan, P. A., 1999, "The Effect of Segment Parameter Error on Gait Analysis Results," Gait and Posture, **9**(3), pp. 173–183.
[47] Rao, G., Amarantini, D., Berton, E., and Favier, D., 2006, "Influence of Body Segments' Parameters Estimation Models on Inverse Dynamics Solutions During Gait," J. Biomech., **39**(8), pp. 1531–1536.
[48] Reinbolt, J. A., Haftka, R. T., Chmielewski, T. L., and Fregly, B. J., 2007, "Are Patient-Specific Joint and Inertial Parameters Necessary for Accurate Inverse Dynamics Analyses of Gait?," IEEE Trans. Biomed. Eng., **54**(5), pp. 782–793.
[49] Riemer, R., Hsiao-Wecksler, E. T., and Zhang, X., 2008, "Uncertainties in Inverse Dynamics Solutions: A Comprehensive Analysis and an Application to Gait," Gait and Posture, **27**(4), pp. 578–588.
[50] Sangole, A., and Levin, M., 2008, "Palmar Arch Dynamics During Reach-to-Grasp Tasks," Exp. Brain Res., **190**(4), pp. 443–452.
[51] Damavandi, M., Barbier, F., Leboucher, J., Farahpour, N., and Allard, P., 2009, "Effect of the Calculation Methods on Body Moment of Inertia Estimations in Individuals of Different Morphology," Med. Eng. Phys., **31**(7), pp. 880–886.
[52] de Leva, P., 1996, "Adjustments to Zatsiorsky-Seluyanov's Segment Inertia Parameters," J. Biomech., **29**(9), pp. 1223–1230.
[53] Hinrichs, R. N., 1990, "Adjustments to the Segment Center of Mass Proportions of Clauser Et Al. (1969)," J. Biomech., **23**(9), pp. 949–951.
[54] Clarys, J. P., and Marfell-Jones, M. J., 1986, "Anatomical Segmentation in Humans and the Prediction of Segmental Masses From Intra-Segmental Anthropometry," Hum. Biol., **58**(5), pp. 761–769.
[55] Clarys, J. P., and Marfell-Jones, M. J., 1986, "Anthropometric Prediction of Component Tissue Masses in the Minor Limb Segments of the Human Body," Hum. Biol., **58**(5), pp. 771–782.
[56] Dizio, P., and Lackner, J. R., 1995, "Motor Adaptation to Coriolis Force Perturbations of Reaching Movements: Endpoint but Not Trajectory Adaptation Transfers to the Nonexposed Arm," J. Neurophysiol., **74**(4), pp. 1787–1792.
[57] Dizio, P., Lathan, C. E., and Lackner, J. R., 1993, "The Role of Brachial Muscle Spindle Signals in Assignment of Visual Direction," J. Neurophysiol., **70**(4), pp. 1578–1584.
[58] Lackner, J. R., and Dizio, P., 1998, "Gravitoinertial Force Background Level Affects Adaptation to Coriolis Force Perturbations of Reaching Movements," J. Neurophysiol., **80**(2), pp. 546–553.
[59] Gomi, H., and Kawato, M., 1997, "Human Arm Stiffness and Equilibrium-Point Trajectory During Multi-Joint Movement," Biol. Cybern., **76**(3), pp. 163–171.
[60] Hollerbach, M. J., and Flash, T., 1982, "Dynamic Interactions Between Limb Segments During Planar Arm Movement," Biol. Cybern., **44**(1), pp. 67–77.
[61] Tee, K. P., Burdet, E., Chew, C. M., and Milner, T. E., 2004, "A Model of Force and Impedance in Human Arm Movements," Biol. Cybern., **90**(5), pp. 368–375.
[62] Perreault, E. J., Kirsch, R. F., and Acosta, A. M., 1999, "Multiple-Input, Multiple-Output System Identification for Characterization of Limb Stiffness Dynamics," Biol. Cybern., **80**(5), pp. 327–337.
[63] Almeida, G. L., Corcos, D. M., and Hasan, Z., 2000, "Horizontal-Plane Arm Movements With Direction Reversals Performed by Normal Individuals and Individuals With Down Syndrome," J. Neurophysiol., **84**(4), pp. 1949–1960.
[64] Sheldon, W., 1940, *The Varieties of Human Physique: An Introduction to Constitutional Psychology*, Harper, New York.
[65] Carter, J. E. L., 2002, *The Heath-Carter Anthropometric Somatotype-Instruction Manual*, San Diego State University, San Diego.
[66] Wilmore, J. H., 1970, "Validation of the First and Second Components of the Heath-Carter Modified Somatotype Method," Am. J. Phys. Anthropol., **32**(3), pp. 369–372.
[67] Lilliefors, H. W., 1967, "On the Komogorov-Smirnov Test for Normality With Mean and Variance Unknown," J. Am. Stat. Assoc., **62**, pp. 399–402.
[68] Weinberg, S. L., and Abramowitz, S. K., 2002, *Data Analysis for the Behavioral Sciences Using Spss*, Cambridge University Press, New York.
[69] Jcgm, 2008, *Evaluation of Measurement Data–Guide to the Expression of Uncertainty in Measurement*, Technical Report No. 100, Joint Committee for Guides in Metrology - Bureau International des Poids et Mesures, Sèvres, France.
[70] Maurel, W., Thalmann, D., Hoffmeyer, P., Beylot, P., Gingins, P., Kalra, P., and Thalmann, N. M., 1996, "A Biomechanical Musculoskeletal Model of Human Upper Limb for Dynamic Simulation," *Proceedings of the Eurographics Workshop on Computer Animation and Simulation '96*, Springer-Verlag, New York, Poitiers, France.
[71] Lee, M. K., Koh, M., Fang, A. C., Le, S. N., and Balasekaran, G., 2009, "Estimation of Body Segment Parameters Using Dual Energy Absorptiometry and 3-D Exterior Geometry," *13th International Conference on Biomedical Engineering*, Springer, Berlin, Heidelberg.
[72] Lee, M. K., Le, N. S., Fang, A. C., and Koh, M. T. H., 2009, "Measurement of Body Segment Parameters Using Dual Energy X-Ray Absorptiometry and Three-Dimensional Geometry: An Application in Gait Analysis," J. Biomech., **42**(3), pp. 217–222.
[73] Schneck, D. J., and Bronzino, J. D., 2003, *Biomechanics: Principles and Applications*, CRC, Boca Raton, FL.
[74] Yamaguchi, G. T., 2001, *Dynamic Modeling of Musculoskeletal Motion*, Kluwer Academic, Dordrecht.